



ELSEVIER

Revealing various coupling of electron transfer and proton pumping in mitochondrial respiratory chain

Fei Sun¹, Qiangjun Zhou³, Xiaoyun Pang^{1,4}, Yingzhi Xu^{1,4} and Ziheng Rao^{1,2}

Cellular respiration is the process that releases energy from food and supplies energy for life processes. The mitochondrial respiratory chain is the final and most important step for cellular respiration and is located on the inner membrane of mitochondrion and comprises four large trans-membrane protein complexes (respiratory chain Complexes I, II, III and IV) as well as ubiquinone between Complexes I/II and III and cytochrome c between Complexes III and IV. The function of mitochondrial respiratory chain is biological oxidation by transferring electrons from NADH and succinate to oxygen and then generating proton gradient across the inner membrane. Such proton gradient is utilized by ATP synthase (ATPase, also called as Complex V) to produce energy molecules ATP. Structural studies of mitochondrial respiratory membrane protein complexes are important to understand the mechanism of electron transfer and the redox-coupled proton translocation across the inner membrane. Here, according to the time line, we reviewed the great achievements on structural studies of mitochondrial respiratory complexes in the past twenty years as well as the recent research progresses on the structures of mitochondrial respiratory supra-complexes.

Addresses

¹National Laboratory of Biomacromolecules, Institute of Biophysics, Chinese Academy of Sciences, Beijing 100101, China

²Laboratory of Structural Biology and Ministry of Education (MOE) Laboratory of Protein Science, School of Medicine and Life Sciences, Tsinghua University, Beijing 100084, China

³Departments of Molecular and Cellular Physiology, Neurology and Neurological Sciences, Structural Biology, Photon Science and Howard Hughes Medical Institute, Stanford University, Stanford, CA 94305, USA

⁴University of Chinese Academy of Sciences, Beijing 100049, China

Corresponding author: Sun, Fei (feisun@ibp.ac.cn)

Current Opinion in Structural Biology 2013, 23:526–538

This review comes from a themed issue on **Membranes**

Edited by **Yigong Shi** and **Raymond C Stevens**

For a complete overview see the [Issue](#) and the [Editorial](#)

Available online 16th July 2013

0959-440X/\$ – see front matter, © 2013 Elsevier Ltd. All rights reserved.

<http://dx.doi.org/10.1016/j.sbi.2013.06.013>

Introduction

Cellular respiration is the process of oxidizing food molecules, like glucose, to carbon dioxide and water and producing the cell's supply of adenosine triphosphate (ATP), used as a source of chemical energy. The process of cellular respiration all occurs in the cytosol of prokaryotes,

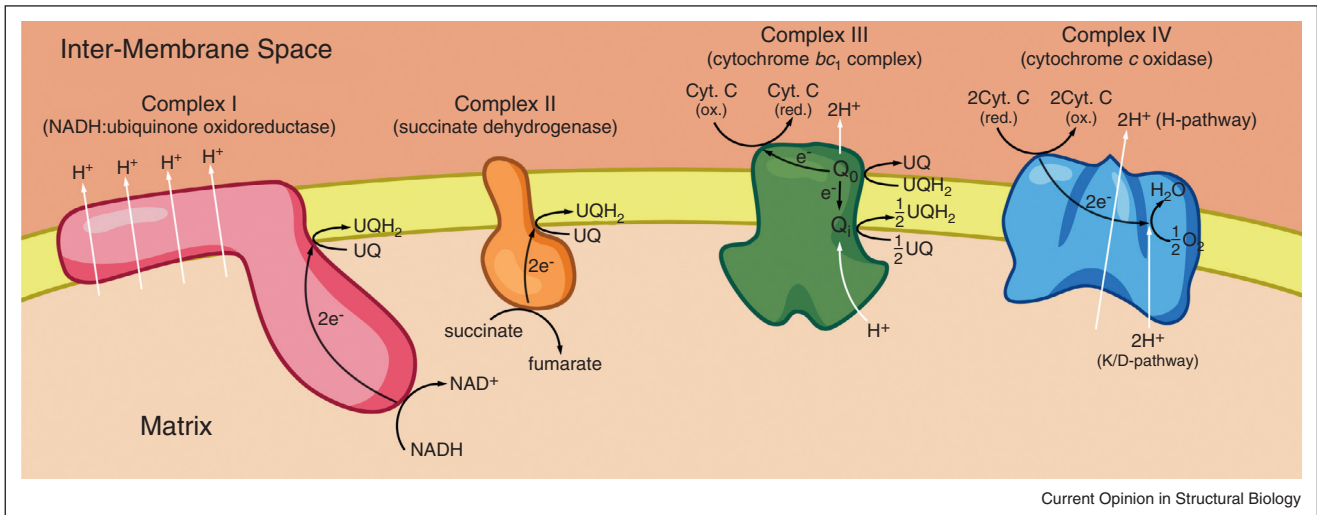
however, mainly takes place in mitochondria of eukaryotic cells.

At the mitochondrial inner membrane in eukaryotes, electrons from the electron donors (such as NADH and succinate) pass through the mitochondrial respiratory chain to the electron acceptor (oxygen) that is reduced to water, accompanying with the pumping of protons across the inner membrane from the matrix to the inter-membrane space (IMS). The mitochondrial respiratory chain comprises four multi-subunit complexes (mitochondrial respiratory Complexes I, II, III and IV) as well as the lipid-soluble electron carrier (ubiquinone, UQ) between Complexes I/II and III and the water-soluble electron carrier (cytochrome c) between Complexes III and IV (Figure 1). Complex I (CI), Complex III (CIII) and Complex IV (CIV) can pump protons from the matrix to IMS and produce an electrochemical proton gradient $\Delta\Psi$ across the inner membrane. The energy of protons flowing back to the matrix will be used by ATP synthesis enzyme (ATPase, also called Complex V) to generate ATP. The coupling between electron transfer and ATP synthesis is called oxidative phosphorylation (OXPHOS) that was well studied in the past century [1–3].

There are two pathways of electron transfer with the mitochondrial respiratory chain (Figure 1). The first one is starting from NADH and electrons of NADH are transferring through CI to UQ, reducing UQ to ubiquinol (UQH₂), then UQH₂ is oxidized by CIII and electrons are transferring through CIII to cytochrome c, and finally cytochrome c is oxidized by CIV by transferring electrons to oxygen to generate water molecule within CIV. The second pathway is coupled with Krebs cycle in the matrix and starting from the oxidation of succinate. Electrons of succinate are transferring to UQ through Complex II (CII), then to cytochrome c through CIII and finally to oxygen through CIV. For the first pathway, each electron transfer is coupled with five protons pumping from matrix to IMS. While, the second one is less effective and each electron transfer will pump three protons from matrix to IMS.

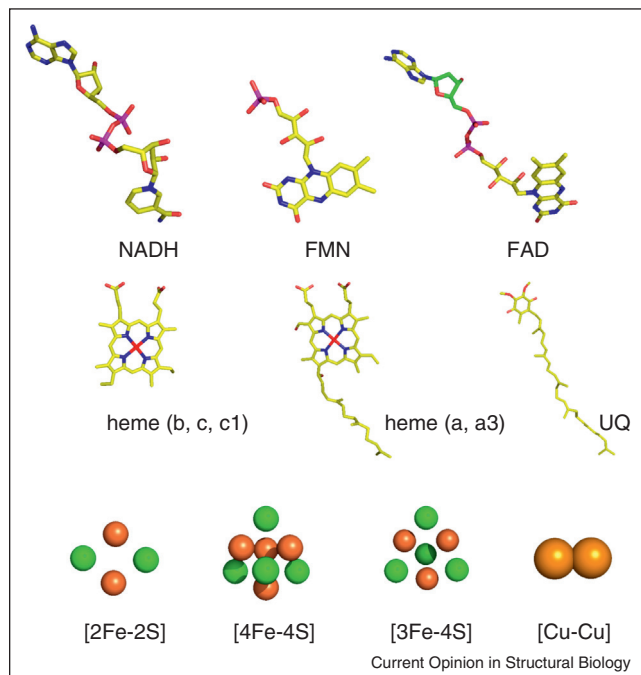
Early purification and biochemical characterization of those membrane protein complexes have revealed most important prosthetic groups (Figure 2) that are involved in the electron transfer pathway, including NADH, FMN, ubiquinone (UQ)/ubiquinol (UQH₂), heme (heme a, heme a₃, heme b, heme c and heme c₁) and iron–sulfur

Figure 1



Schematic diagram of electron transfer and proton translocation within mitochondrial respiratory complexes at the inner membrane. All the information is based on the latest structural research of mitochondrial respiratory complexes. Mitochondrial inner membrane is colored in yellow, matrix in light salmon and inter-membrane space in salmon. Mitochondrial respiratory Complex I (NADH:ubiquinone oxidoreductase) is colored in red, Complex II (succinate dehydrogenase) in orange, Complex III (bc1 complex) in green and Complex IV (cytochrome c oxidase) in blue. The electron transfer pathways within each complex as well as the coupled proton translocations are indicated by black and white arrows, respectively. NADH, dihydronicotinamide; UQ, ubiquinone; UQH₂, ubiquinol; cyt. c (ox.), cytochrome c in oxidized state; cyt. c (red.), cytochrome c in reduced state.

Figure 2

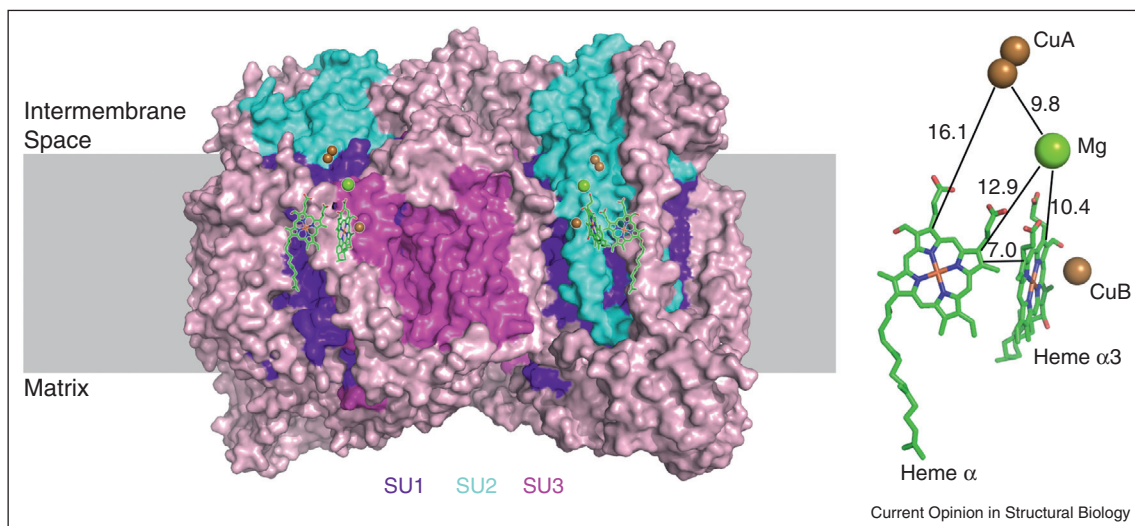


The structures of prosthetic groups in the mitochondrial respiratory chain. NADH, reduced form of nicotinamide-adenine dinucleotide; FMN, flavin mononucleotide; FAD, flavin adenine dinucleotide; UQ, ubiquinone. NADH, FMN, FAD, heme groups and UQ are shown in ball-and-sticks. The iron-sulfur clusters and Cu center are shown in sphere. The atoms are colored with the scheme, carbon in yellow, nitrogen in blue, oxygen in red, phosphorus in magenta, sulfur in green, iron in salmon and copper in gold.

clusters (Fe₂S₂, Fe₄S₄ and Fe₃S₄) as well as some metal centers (e.g. Cu center). Those prosthetic groups are bound with or buried in the respiratory complexes and have different redox potentials that are also affected by the binding environment of them. Quantum mechanics computation had indicated that the electrons can directly transfer between the prosthetic groups only if their edge-to-edge distance is shorter than 14 Å [4^{••}]. The electron transfer direction and efficiency will therefore be determined by the redox potential of prosthetic groups. However, the electron transfer pathway within each mitochondrial respiratory complex and its coupling with the proton translocation across the inner membrane had been mysterious for many years before the structural studies of those complexes became available.

In the past twenty years, structural studies of mitochondrial respiratory complexes as well as their prokaryotic counterparts have essentially revealed the organization of those embedded prosthetic groups and the electron transfer pathway within the complexes and disclosed different coupling ways between electron transfer and proton pumping across the inner membrane. Here we will review the structural studies of mitochondrial respiratory complexes and summarize the various coupling mechanisms between electron transfer and proton pumping. At the end, we will also discuss the recent research progresses about the respiratory supra-complexes, which will shed new insights into the electron transfer within the mitochondrial respiratory chain.

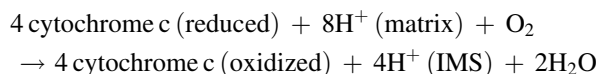
Figure 3



Surface representation of dimerized bovine mitochondrial respiratory Complex IV structure (left, PDB code: 1OCC) and the spatial arrangement of its prosthetic groups (right). The membrane region is shown as gray box. The embedded prosthetic groups (left) are shown in sticks for heme groups and spheres for ion clusters, and superimposed on the surface of Complex IV to indicate their relative spatial position. The edge-to-edge distances of prosthetic groups are indicated accordingly (right). The core subunits of Complex IV, SU1, SU2 and SU3, are colored and labeled as indicated.

Direct redox-coupled proton translocation within Complex IV

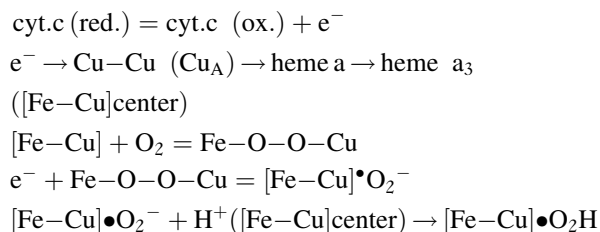
The first breakthrough of structural studies of mitochondrial respiratory complexes occurred in 1995, when the crystal structures of both prokaryotic cytochrome *c* oxidase and bovine mitochondrial respiratory Complex IV (CIV) were determined [5[•],6]. CIV, also known as cytochrome *c* oxidase (EC 1.9.3.1), is the end-point of the mitochondrial respiratory chain. It receives four electrons from four cytochrome *c* molecules reduced by CIII and transfers them to one oxygen molecule and generates two water molecules by consuming four protons in matrix side (Figure 1). At the same time, four protons in matrix are transported into IMS. The total reaction is shown below.



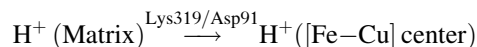
In 1995, Iwata *et al.* solved the 2.8 Å crystal structure of the antibody bound prokaryotic cytochrome *c* oxidase from *Paracoccus denitrificans*, revealing the mini-version of mitochondrial CIV in the first time [5[•]]. In 1996, Tsukihara *et al.* solved the crystal structure of the complete bovine mitochondrial CIV that appeared as a dimer and possesses 28 trans-membrane helices [7^{••}]. Bovine CIV, with total molecular weight 210 kDa, contains 13 subunits and three of them (called SU1, SU2 and SU3) form the core of CIV (Figure 3). SU1 has two heme centers (heme *a* and *a*₃) and a Cu center (Cu_B). Heme *a*₃ and Cu_B form a binuclear center that is the site for oxygen reduction. SU2 possesses another Cu center (Cu_A) with two Cu atoms and accepts the electron donation

from cytochrome *c*. SU3 has seven trans-membrane helices and interacts with SU1. Besides SU1, SU2 and SU3, other subunits of bovine CIV surround the core and stabilize the whole complex. The genes of SU1, SU2 and SU3 are coded by mitochondrial DNA and are conserved in comparison with their prokaryotic counterparts [7^{••}]. Further structural studies of cytochrome *c* oxidase [5[•],6,7^{••},8,9,10^{••},11,12,13^{••}] afterwards have clearly revealed the electron transfer pathway (Figures 1 and 3) within CIV as shown below.

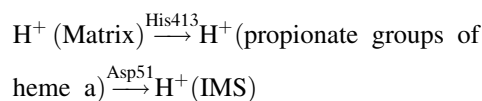
Electron transfer:



Chemical proton delivery via K/D pathway:



Redox-coupled proton translocation via H-pathway:



The electrons from cytochrome *c* are transferred through a set of prosthetic group to the heme a_3 site where the oxygen molecule is captured by [Fe–Cu] center and reduced. At the same time, the protons from matrix are pumped to IMS. Obviously, there should be two proton-pathways within CIV. One is going from matrix to the heme a_3 site and consumed by oxygen reduction. Another one is going from matrix to IMS for proton translocation. Iwata *et al.* proposed two proton pathways, called K-pathway and D-pathway, according to the structure of prokaryotic cytochrome *c* oxidase [5^{*}]. It was proposed that the K-pathway delivers protons, via Lys354, from matrix going to the binuclear center for water molecule generation and the D-pathway conducts protons, via Asp124 from the matrix side to Glu278 near heme a_3 , where the protons are directed to the binuclear center or routed to a postulated proton loading site before releasing to IMS [5^{*},8,9,14]. In this model, heme a_3 takes a key role, via its propionate groups, for vectorial proton translocation across the membrane.

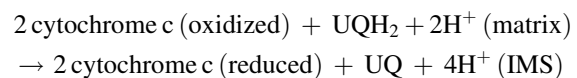
However, extensive structural studies of mitochondrial CIV in reduced, oxidized and inhibitor bound state as well as their mutants [10^{**},13^{**},15–17] confirmed the existence of both K-pathway (Lys319) and D-pathway (Asp91) but disagreed the role of heme a_3 for proton translocation. According to the crystal structures of CIV, the third proton pathway, H-pathway, containing His413 at the matrix side and Asp51 at the IMS side, was proposed [9,13^{**}]. In this model, the low-spin heme *a* takes the role for proton pumping across the membrane and the redox state conversion of heme *a* drives the significant conformational changes of the subunit SU1 and heme *a* itself, gating the proton delivery from matrix side and its release to IMS side [9,13^{**}]. This model had been further investigated and agreed with computational studies [18] and experimental evidences [19,20]. Especially, the recent H/D exchange resonance Raman spectroscopic experiments revealed that it is the propionate groups of heme *a* not heme a_3 that response the redox changes actively [20], suggesting the unique role of heme *a* for redox-coupled proton translocation. The biological importance of D-pathway was also evaluated in the mitochondrial CIV by investigating the conformational changes of His503 that is at the entrance of D-pathway and close to Asp91 [15]. As a result, we may propose that both K-pathway and D-pathway are responsible for delivering chemical protons to the bi-nuclear center for consumption and only the H-pathway allows protons from matrix pumping to IMS (Figure 1), which is directly coupled to the redox conversion of heme *a*.

The important residue Asp51 for proton translocation in H-pathway of mitochondrial CIV is not conserved in prokaryotic cytochrome *c* oxidase. Furthermore, recent

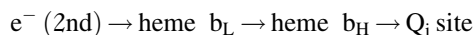
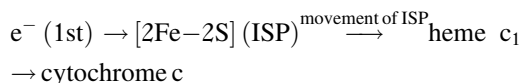
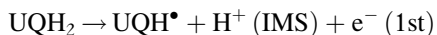
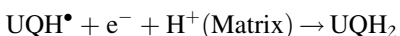
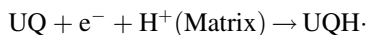
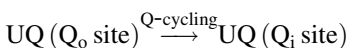
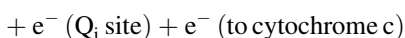
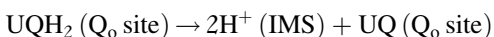
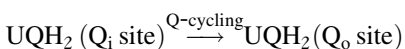
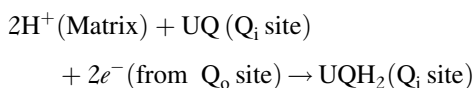
theoretical computation [21] and spectrometric data [22] upon prokaryotic cytochrome *c* oxidase support the role of D-pathway for proton translocation. Therefore, the molecular details of the coupling between electron transfer and proton pumping in mitochondrial CIV still needs more investigation and that whether such kind of mechanism is evolutionary conserved from prokaryotic cytochrome *c* oxidase to eukaryotic version is awaiting the final answer.

Q-cycle mechanism for proton translocation within Complex III

The second breakthrough of structural studies of mitochondrial respiratory complexes occurred in 1997 and 1998, when the crystal structures of mitochondrial respiratory Complex III (CIII) from bovine, chicken or rabbit hearts were determined [23,24^{**},25^{**}]. CIII (EC 1.10.2.2), also known as ubiquinol-cytochrome *c* oxidoreductase or bc1 complex, is the hub of the mitochondrial respiratory chain, passing electrons from CI and CII to CIV. It catalyzes the reduction of cytochrome *c* by oxidation of ubiquinol that is produced by CI and CII, and couples the proton translocations across the mitochondrial inner membrane (Figure 1). Four proton translocations are coupled with two electron transfers. The total reaction is shown below.



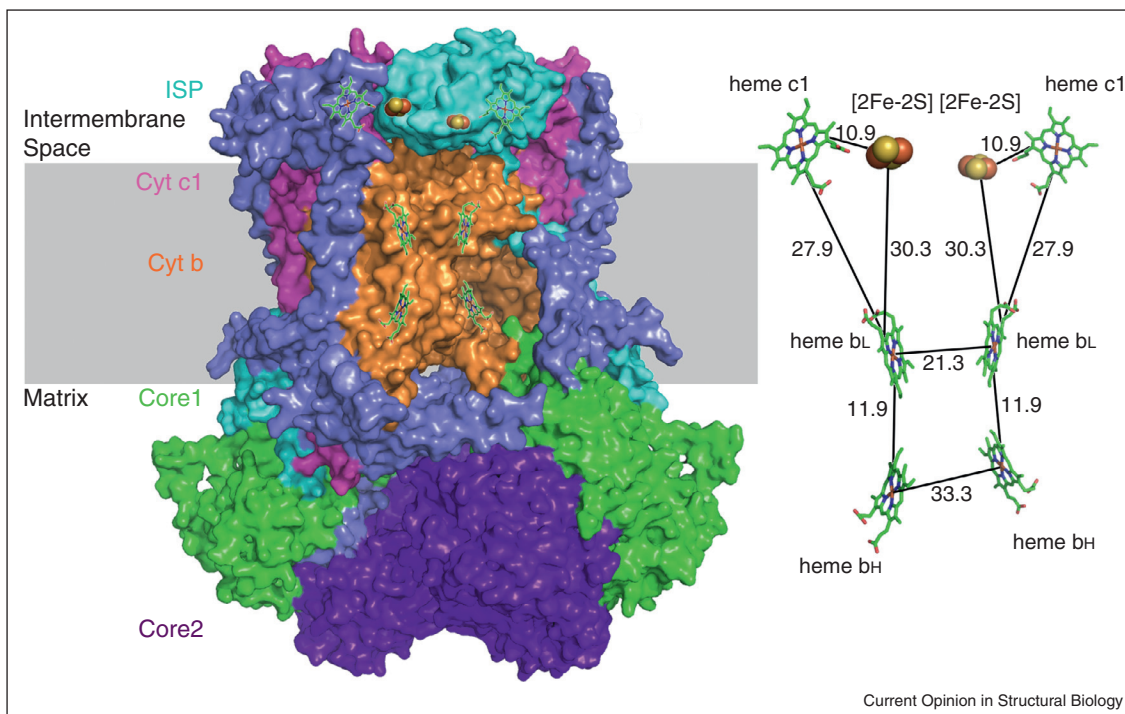
In 1997, Xia *et al.*, for the first time, reported the crystal structure of partial CIII from bovine heart mitochondrion based on 2.9 Å diffraction data [23]. One year later, Zhang *et al.* solved crystal structures of CIII from chicken, bovine and rabbit heart mitochondrion at 3.0 Å as well as the crystal structures bound with inhibitors [25^{**}]. At the same year, Iwata *et al.* solved the complete crystal structure of the bovine heart mitochondrial CIII at 2.8 Å [24^{**}]. Within Iwata's structure, bovine CIII, with total molecular weight 240 kDa, contains 11 subunits and forms a physiological dimer (Figure 4). Each CIII monomer has one cytochrome *b* subunit containing heme b_H (its maximum absorption wavelength is 562 nm) and heme b_L (its maximum absorption wavelength is 566 nm), one cytochrome c_1 subunit containing heme c_1 and one iron–sulfur cluster binding protein (ISP, also called Rieske protein) containing one [2Fe–2S] cluster. These three subunits form the core of CIII and carry out the electron transfer and redox-coupled proton translocation. In 2002, Lange *et al.* reported the crystal structure of CIII bound with cytochrome *c* and found that the CIII dimer only binds one cytochrome *c* each time [26^{*}]. The above crystal structures as well as the following structural studies of CIII bound with UQ/inhibitors [27–30] have provided a comprehensive understanding of the mechanism of electron transfer and proton translocation coupling within CIII, which is shown below.

Electron transfer at Q_o site (proximal to IMS):**Electron transfer at Q_i site (proximal to Matrix):****Coupled proton translocation by Q-cycling:**

There are two UQ binding sites found within CIII. One site is proximal to the matrix side and called as Q_i site, where UQ is reduced to UQH₂. Another site is close to the IMS and called as Q_o site, where UQH₂ is oxidized to UQ. Both Zhang's and Iwata's structures revealed three kinds of ISP conformations, one of which is close to the Q_o site, the second one is close to the cytochrome c₁ subunit and the third one has the intermediate conformation in between. At the intermediate conformation (Figure 4), the edge-to-edge distances between heme c₁ and heme b_L, between heme c₁ and [2Fe-2S] and between heme b_L and [2Fe-2S] are all far away than 14 Å, indicating no direct electron transfer occurred among those prosthetic groups. The movement of ISP is therefore mandatory for the electron transfer within CIII. Xia's research group studied many UQ/inhibitors bound CIII structures [27,28] and had observed that the different positions of ISP were correlated with the conformational changes of cytochrome b subunit, indicating the redox-driven movement of ISP [30].

As a result, the electron transfer of CIII is tightly correlated with the redox-driven movement of ISP. The UQH₂ is oxidized at the Q_o site with one electron transferring to the cytochrome c via movement of ISP

Figure 4



Surface representation of dimerized bovine mitochondrial respiratory Complex III structure (left, PDB code: 1BE3) and the spatial arrangement of its prosthetic groups (right). The membrane region is shown as gray box. The embedded prosthetic groups (left) are shown in sticks for heme groups and spheres for iron-sulfur clusters, and superimposed on the surface of Complex III to indicate their relative spatial position. The edge-to-edge distances of prosthetic groups are indicated accordingly (right). The catalytic subunits of Complex III, ISP (iron sulfur protein), Cyt c₁ (cytochrome c₁) and Cyt b (cytochrome b), are colored and labeled as indicated. The subunits Core1 and Core2, which are important for the assembly of Complex III and take the role as the mitochondrial processing peptidase, are colored and labeled.

and heme c_1 and the second electron transferring to the Q_i site via heme b_L and heme b_H . At the Q_i site, the UQ is reduced to UQH₂. The newly reduced UQH₂ will go into the Q-pool [31] and be recycled to Q_o site for oxidation, which is called Q-cycle [32,33]. In each cycle, one reduction of UQ at Q_i site is coupled with two oxidations of UQH₂ at Q_o site by consuming two protons from matrix and releasing four protons to IMS. The net result is pumping protons from matrix to IMS and forming a proton gradient across the inner membrane. In each Q-cycle, there are two electrons transferred from UQH₂ to two molecules of cytochrome *c*. As a result, the proton translocation and electron transfer within CIII are coupled with a redox-driven Q-cycle mechanism.

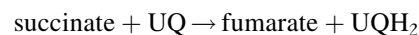
One thing has to be noted that the detailed mechanism of how electron is transferred from heme c_1 to cytochrome *c* was further addressed from higher resolution (1.9 Å) crystal structure of yeast mitochondrial CIII bound with cytochrome *c* in reduce state [34].

Although it is clear that the coupling between electron transfer and proton translocation in CIII is carried out by Q-cycle mechanism, the molecular details are still not clear enough. There could be a couple of electron transfer short circuits occurred within the above Q-cycle mechanism, for example, both electrons of UQH₂ at the Q_o site can be transferred to the cytochrome *c* sequentially instead of bifurcating one electron to the Q_i site, forming a short circuit [35^{*}]. Therefore, the current most important unsolved question is how the short circuits be avoided during the Q-cycle. Recently, different models including single-gated model [35^{*}], double-gated model [4^{**},35^{*}] and activated Q-cycle model [36] have been proposed to explain how the nature couples electron transfer and proton translocation efficiently without forming a short circuit. Interestingly, however, theoretical computation and simulation by Smirnov and Nori suggested the bifurcation of the electron pathways at the Q_o site occurs naturally, without any additional gates [37]. And moreover, a disabled Q_i site does not completely inhibit electron transfer and proton translocation within cytochrome b_6f (a homologous complex to bc_1 complex in photosynthetic system), suggesting a bypassing mechanism existing beside the Q-cycle mechanism [38]. Therefore, the coupling mechanism within mitochondrial CIII is still in a very active research.

Electron transfer within Complex II and the proton production in matrix

The third breakthrough of structural studies of mitochondrial respiratory complexes occurred in 2003, when the crystal structure of the prokaryotic version of mitochondrial respiratory Complex II (CII), *Escherichia coli* succinate-ubiquinone oxidoreductase (SQR), was determined at 2.6 Å [39^{*}]. However, the crystal structures of real mitochondrial CII from porcine heart at

2.4 Å [40^{**}] and avian heart at 2.1 Å [41] became available in 2005. Mitochondrial respiratory CII (EC 1.3.5.1), also called as succinate dehydrogenase or succinate-ubiquinone (SQR), is the only enzyme that participates in both the citric acid cycle (Krebs cycle) and the mitochondrial electron transfer chain and has been raised more attentions due to its high potency of being a novel target for anti-cancer agents [42]. CII catalyzes the oxidation of succinate to fumarate with the reduction of UQ to UQH₂ (Figure 1). There is no proton translocation across the inner membrane during the electron transfer within CII. The total reaction catalyzed by CII is shown below.



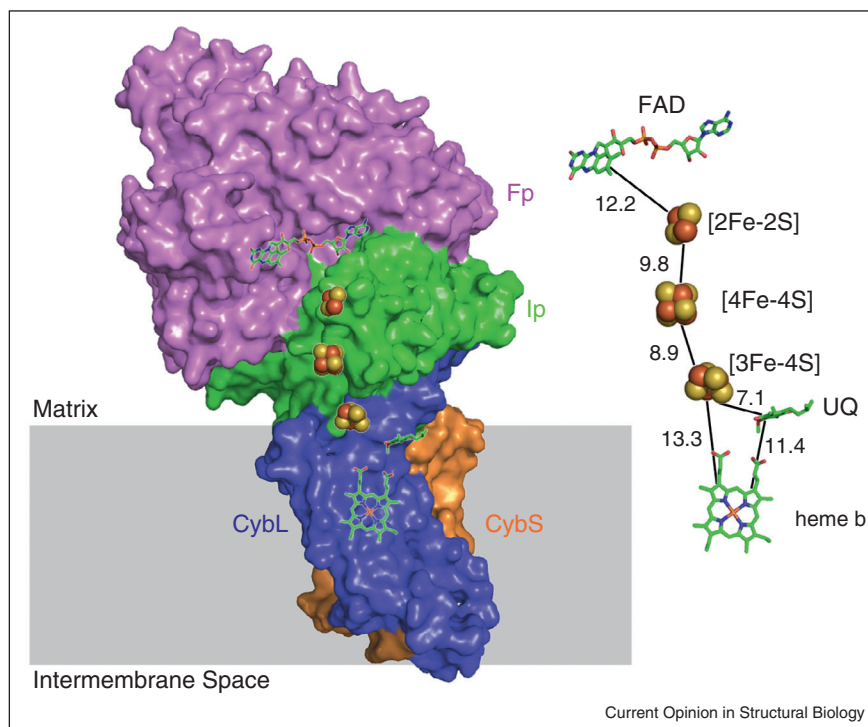
Before the structural information of mitochondrial CII became available, the structures of bacterial ubiquinol fumarate oxidoreductases (QFR), members of SQR superfamily, were firstly determined, including the complete *E. coli* QFR at 3.3 Å resolution [43] and the *Wolinella succinogenes* QFR at 2.2 Å resolution [44] in 1999. In 2003, Yankovskaya *et al.* solved the crystal structure of *E. coli* SQR at 2.6 Å resolution [39^{*}]. In 2005, Sun *et al.* reported the crystal structure of mitochondrial CII from porcine heart at 2.4 Å resolution [40^{**}] and Huang *et al.* presented the highest resolution (2.1 Å) crystal structure of mitochondrial CII from avian heart [41]. Comparisons among these solved structures of SQR superfamily members revealed their highly conserved hydrophilic parts and varieties of transmembrane parts from prokaryotic version to eukaryotic mitochondrial CII [40^{**},45].

Mitochondrial CII consists of a soluble catalytic heterodimer and an integral transmembrane region (Figure 5). The soluble catalytic heterodimer is made up of flavo-protein (Fp or SdhA) with a covalently bound FAD cofactor and an iron-sulfur protein (Ip or SdhB) containing three Fe-S clusters, [2Fe-2S], [4Fe-4S] and [3Fe-4S]. The integral transmembrane region anchoring the complex to the inner membrane contains two hydrophobic subunits (CybL and CybS) with one heme *b* prosthetic group embedded. The UQ binding site is formed by Ip, CybL and CybS, proximal to the matrix side and further studied from the structures of CII bound with UQ reduction inhibitors, including carboxin [41,46], atpenin A5 [47], 2-thenpyltrifluoroacetone (TTFA) [40^{**},41], dinitrophenols [39^{*},48], pentachlorophenol [46,49], dinitrophenol, 2-heptyl-4-hydroxyquinoline-*N*-oxide [48] and thiabendazole [49].

The above various structural studies of CII and CII bound with substrate and inhibitors had provided a well understanding of the electron transfer within CII as shown below.

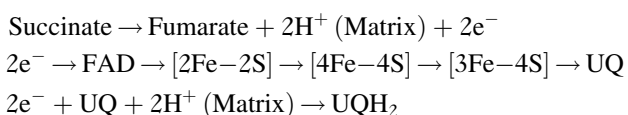
In brief, the succinate is dehydrogenated to fumarate at the dicarboxylate-binding site of Fp, generating two

Figure 5



Surface representation of porcine mitochondrial respiratory Complex II structure (left, PDB code: 1Z0Y) and the spatial arrangement of its prosthetic groups (right). The membrane region is shown as gray box. The embedded prosthetic groups (left) are shown in sticks for heme, FAD and UQ groups and spheres for iron–sulfur clusters, and superimposed on the surface of Complex II to indicate their relative spatial position. The edge-to-edge distances of prosthetic groups are indicated accordingly (right). The hydrophilic subunits Fp (flavoprotein) and Ip (iron–sulfur protein), and the transmembrane subunits CybL (cytochrome b protein L) and CybS (cytochrome b protein S) are colored and labeled accordingly.

Electron transfer:



protons at the matrix side. Two electrons from one succinate molecule are extracted by FAD and transferred to the UQ binding site by passing through three iron–sulfur cluster, [2Fe–2S], [4Fe–4S] and [3Fe–4S]. At the UQ binding site, UQ is reduced to UQH₂, by consuming two protons at the matrix side. The net result from succinate oxidation and UQ reduction does not change the proton concentration of the matrix and generate the proton gradient across the inner membrane.

One thing should be noted that the prosthetic group heme b embedded within the transmembrane helices of CII does not appear in the above electron transfer pathway, although the distances between heme b and [3Fe–4S] and between heme b and UQ are feasible for electron transfers among them (Figure 5). The role of heme b group for the function

of *E. coli* SQR was suggested by Yankovskaya *et al.* that it provides a site for electron-sink and reduces the reactive oxygen species (ROS) productions at the FAD and iron–sulfur cluster sites [39[•]]. However, such mechanism would be not true for mitochondrial CII because the redox potential of mitochondrial CII heme b group is much lower than that of *E. coli* SQR [40^{••},50]. As a result, the role of heme b group in mitochondrial CII still needs further investigation in the future.

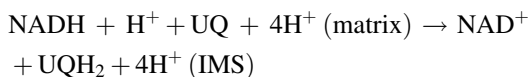
The second thing should be noted that the crystal structure of porcine CII bound with TTFA suggested two UQ binding sites, one in the proximal side and another in the distal side [40^{••}]. However, the higher resolution crystal structure of avian CII bound with TTFA did not show TTFA bound at the distal site [41]. If there was the second UQ binding site at the distal side, whether it is the oxidation site or reduction site, the net result from CII catalysis would yield a proton gradient across the inner membrane and thus endow CII the function of proton pumping similar to CIII, which, however, should not be true according to the current research data of CII. The rational explanation would be that two TTFA molecules observed from the structure of porcine CII co-crystallized with TTFA [40^{••}] did indicate two high affinity TTFA

binding sites, one is superimposed with the UQ binding site and another one is at the distal side, which, however, did not indicate the second UQ binding site.

Indirect redox-coupled proton translocation within Complex I by allosteric conformational changes

The latest breakthrough of mitochondrial respiratory complexes study occurred in recent years (2006–2013), especially in 2013, when the high-resolution (3.3 Å) structures of prokaryotic version of mitochondrial respiratory Complex I (CI) became available [51[•],52,53,54^{••}]. The median resolution (6.3 Å) electron density map of mitochondrial respiratory CI from yeast was also reported in 2010 while its atomic model from higher resolution data is under awaiting [55]. As the most complicated complex within mitochondrial respiratory chain, the determination of the structure of CI is a big challenge and has been becoming the milestone of this field.

Mitochondrial respiratory CI (EC 1.6.5.3), also referred as NADH:ubiquinone oxidoreductase or NADH dehydrogenase, is the first enzyme of the respiratory chain and plays a central role in cellular energy production and its dysfunction is related with many human neurodegenerative diseases [56,57]. CI is the main electron entry point in the respiratory electron transfer chain and catalyzes the transfer of two electrons from NADH to UQ and the redox-coupled translocation of four protons across the inner membrane (Figure 1). The total reaction catalyzed by CI is shown below.



CI is the largest and most complicated enzyme of the respiratory chain. Mammalian CI comprises of 44 different subunits with molecular weight ~980 kDa [58,59]. The prosthetic groups, one non-covalently bound flavin mononucleotide (FMN) and eight iron–sulfur clusters, are embedded within the hydrophilic part of CI. There are seven transmembrane subunits (ND1–ND6 and ND4L) that are encoded by the mitochondrial DNA while all the other subunits are encoded by nuclear genes, translated in cytoplasm and imported into the mitochondrion [60]. Bacterial NADH dehydrogenase (NDH-1) is a mini-version of mitochondrial CI and comprises of 13–16 subunits with molecular weight ~550 kDa in total [54^{••},61]. The assembly of these subunits is sufficient for the complete CI function and conserved from bacterial to human [62–64]. In mammalian mitochondrial CI, besides the 14 core subunits conserved to their prokaryotic counterparts, the rest ~30 subunits, referred as accessory (or supplementary) subunits, are also essential for the assembly and stability of CI [58,65–67].

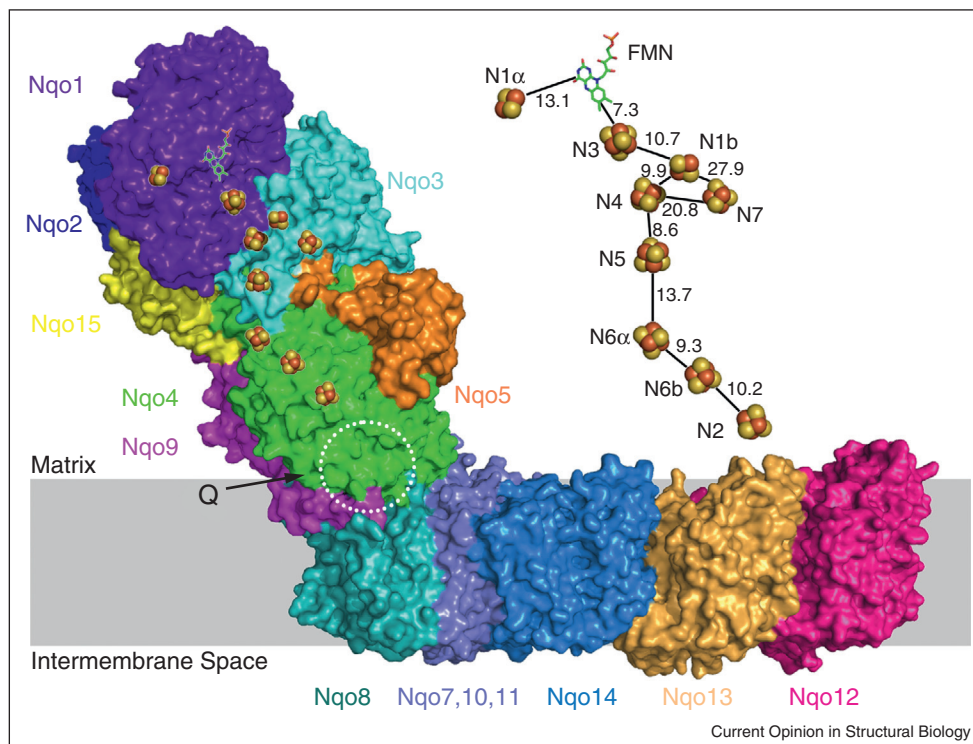
The early structural studies of prokaryotic and eukaryotic CI were performed using electron microscopy

approaches. Electron microscopic single particle analyzes of CI from bacteria *Aquifex aeolicus* [68] and *E. coli* [61,69,70], from fungus *Neurospora crassa* [71–73] and *Yarrowia lipolytica* [74], and from mammalian *Bos taurus* [75,76] have all revealed that CI shares a conserved L-shape and consists of two major segments. One is the hydrophobic domain embedded in the inner membrane and another is the hydrophilic ‘arm’ protruding into the matrix.

The structural information revealed by electron microscopy was later supported by the crystallographic analysis of CI from *Yarrowia lipolytica* [55], *E. coli* [52] and *Thermosus thermophilus* (Figure 6) [52,77]. The first crystal structure (3.3 Å) of the hydrophilic part of CI from *Thermosus thermophilus* was determined in 2006 by Sazanov *et al.* [51[•]]. This sub-complex contains all the redox centers including one FMN, one Fe–S cluster (N1a), one [2Fe–2S] cluster (N1b) and seven [4Fe–4S] clusters (N2, 3, 4, 5, 6a, 6b and 7) (Figure 6). The main electron transfer pathway of CI was also revealed for the first time from this structure. Thereafter, Sazanov’s group reported the architecture of the hydrophobic part of CI from *E. coli* at 3.9 Å in 2010 [52] and 3.0 Å resolution in 2011 [53]. This sub-complex is slightly curved both in plane and in perpendicular to membrane surface with the length of 160 Å and thickness of 40 Å. The structure revealed three large subunits, NuoL, NuoM and NuoN, each of which is the homolog of Na⁺/H antiporter and contains 14 conserved transmembrane helices, suggesting that these three subunits are responsible for the putative proton-translocation pathways of CI. Most surprisingly, the membrane subunit NuoL contains a very long (110 Å) amphipathic α-helix, spanning almost the entire length of the hydrophobic part of CI, which probably couples the electron transfers and the allosteric conformational changes of proton channels within NuoL, NuoM and NuoN. The subsequent crystal structures of entire CI from *Thermosus thermophilus* at 4.5 Å resolution [52] and from *Yarrowia lipolytica* at 6.3 Å [55] also confirmed the above discoveries.

Recently, Sazanov’s group determined the 3.3 Å resolution crystal structure of the entire CI from *Thermosus thermophilus* [77], giving the most clear view of this complicated complex in atomic level. This complex (molecular weight 536 kDa) consists of 16 different subunits with 64 transmembrane helices and nine iron–sulfur clusters (Figure 6). Unlike Nqo12, Nqo13 and Nqo14 (NuoL, NuoM and NuoN in *E. coli*), the subunit Nqo8 does not form an antiporter-like channel but interacts with the subunits Nqo10 and Nqo11 together to coordinate the fourth proton-translocation pathway, called as E-channel [77]. With this complete structure of the whole CI, the UQ binding site was clearly found near N2 prosthetic group with a long (30 Å) and narrow (~5 Å) chamber at the interface of subunits Nqo4, Nqo6 and

Figure 6

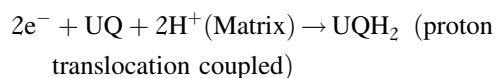
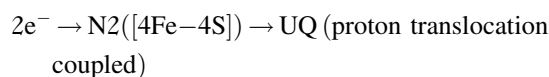
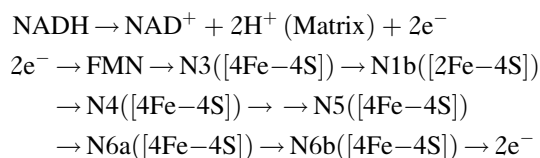


Surface representation of mitochondrial respiratory Complex I structure from *Thermus thermophilus* (left, PDB code: 4HEA) and the spatial arrangement of its prosthetic groups (right). The membrane region is shown as gray box. The embedded prosthetic groups (left) are shown in stick for FMN group and spheres for iron-sulfur clusters, and superimposed on the surface of Complex I to indicate their relative spatial position. The edge-to-edge distances of prosthetic groups are indicated accordingly (right). The putative UQ binding formed by subunits Nqo4, Nqo9 and Nqo8 is indicated with a dashed white circle. The subunits Nqo1-5, Nqo9 and Nqo15 of the hydrophilic arm of Complex I, and the subunits Nqo7, Nqo8 and Nqo10-14 of the hydrophobic domain of Complex I are colored and indicated accordingly. The subunits Nqo6 and Nqo16 of the hydrophilic arm are located on the back and not shown. There are four putative proton translocation pathways via the antiporter-like subunits Nqo12, Nqo13 and Nqo14 and the E-channel formed by subunits Nqo8, Nqo10 and Nqo11.

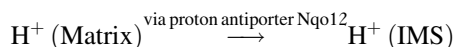
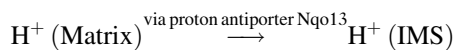
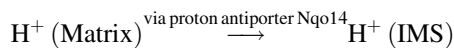
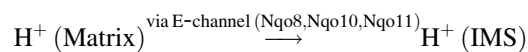
Nqo8. It was suggested that a sealed and out-of-membrane UQ binding chamber could enable the redox-driven conformational changes propagate to the four proton-translocation channels, resulting in the translocation of four protons per cycle of electron transfers.

As a result, the current structural information of prokaryotic CI has proposed a rational model for the electron transfer within CI and its coupled proton translocation via allosteric conformational changes, which is described as below (using the nomenclatures of CI from *Thermos thermophiles*, see also Figure 6).

Electron transfer:



Proton translocation via allosteric conformational changes:



Before the detailed crystal structure of the whole CI became available, people have proposed various models about the coupling mechanism of CI, including the chimeric model by Ohnishi *et al.* [78,79], based on the

assumption of the existence of two ubiquinone-binding sites in bovine mitochondrial CI [80]; the two-state model by Brandt, hypothesizing that the conformational changes are coupled with each electron transfer and induce every two proton translocations [81]; and the single-step reversible mechanism by Efremov and Sazanov, showing four putative proton channels and predicting that the negative electric charge of the anionic ubiquinol head group is a major driving force for conformational changes [66,82^{*}]. The very recent resolved crystal structure of entire CI from *Thermosus thermophilus* [77] has shown more agreements with the single-step reversible coupling mechanism. However, the molecular details of this coupling mechanism needs more investigations and many questions, such as how the redox in the N2 cluster is coupled to the reduction of ubiquinone to generate conformational changes and how these changes transmit into an 'allosteric mechanism' and activate the antiporters domains, are sitting on the frontier of the field.

New insights from the structural studies of respiratory supercomplexes

Several lines of evidence have recently replaced the random diffusion model of electron transfer with a model of supra molecular organization based on specific interactions between individual respiratory complexes. The mitochondrial respiratory chain complexes might interact to form supra molecular assemblies termed as respiratory supercomplexes or respirasomes [83–85]. Most of these supercomplexes were isolated by sucrose gradient centrifugation and identified (or purified) by native gel electrophoresis including blue Native PAGE [86] and clear Native PAGE [87] and their structures were studied by single particle electron microscopy.

The supercomplex CI + CIII₂ + CIV isolated from bovine heart mitochondria [84,88,89^{*},90^{*}] is one of the most intriguing supercomplexes because it contains all the redox enzymes required for the complete electron transfer pathway from NADH to oxygen. Besides, the supercomplexes such as CI + CIII₂ [85,91] and CIII₂ + -CIV₁₋₂ [92] were also identified. In 2007, Schafer *et al.* presented the first 3D map of a respiratory chain supercomplex CI + CIII₂ + CIV from bovine heart mitochondria [88]. Recent higher resolution (~2 nm) cryo-electron microscopic reconstructions of bovine mitochondrial CI + CIII₂ + CIV by Althoff *et al.* [89^{*}] and Dudkina *et al.* [90^{*}] have revealed much more details of how these respiratory complexes being organized together for the more efficient electron transfer. It was also demonstrated that the supra molecular assembly of the individual complexes strongly depends on the membrane lipid content and composition [93]. The existence of the respiratory supercomplexes raised a new challenge for understanding the mechanism of the electron transfer and proton translocation coupling through the mitochondrial respiratory chain [94], which needs more structural work in the future.

Concluding remarks

In the past twenty years, there were great achievements on the structural studies of mitochondrial respiratory complexes and those available structures have open the door of understanding the molecular details of the coupling between electron transfer and proton translocation, which is the central theme of understanding how efficient the nature transforms energy. Although we have realized various coupling mechanisms, their molecular details are still under debating and remain a very active of researches. The detailed conformational changes of CI upon different redox states and with ubiquinone/ubiquinol species bound are waiting to be observed. The high-resolution structure of the real version mitochondrial CI is also greatly expected in the near future. More experimental data need to be collected to further confirm the physiological role of H-pathway in CIV. The understanding of how CIII avoids a short circuit during its Q-cycle needs a refreshing. In addition, the high-resolution structures of respiratory supercomplexes are even more important in the future to understand the integral coupling mechanism within the mitochondrial respiratory chain.

Acknowledgements

We apologize to the scientists whose contributions were not cited because of space limitations. This work was supported by grants from the Chinese Ministry of Science and Technology (2011CB910301) and the National Natural Science Foundation of China (31030023).

References and recommended reading

Papers of particular interest, published within the period of review, have been highlighted as:

- of special interest
- of outstanding interest

1. Mitchell P: **Coupling of phosphorylation to electron and hydrogen transfer by a chemi-osmotic type of mechanism.** *Nature* 1961, **191**:144-148.
2. Mitchell P: **Chemiosmotic coupling in oxidative and photosynthetic phosphorylation.** *Biol Rev Camb Philos Soc* 1966, **41**:445-502.
3. Saraste M: **Oxidative phosphorylation at the fin de siecle.** *Science* 1999, **283**:1488-1493.
4. Osyczka A, Moser CC, Daldal F, Dutton PL: **Reversible redox energy coupling in electron transfer chains.** *Nature* 2004, **427**:607-612.
Theoretical studies of electron transfer mechanism, revealing a significant tunnel effect of electrons between two prosthetic groups if their edge-to-edge distance is shorter than 14 Å, providing the theoretical framework for the study of electron transfers.
5. Iwata S, Ostermeier C, Ludwig B, Michel H: **Structure at 2.8 Å resolution of cytochrome c oxidase from *Paracoccus denitrificans*.** *Nature* 1995, **376**:660-669.
The first crystal structure of the prokaryotic version of Complex IV, suggesting two proton pathways, the K-pathway and D-pathway.
6. Tsukihara T, Aoyama H, Yamashita E, Tomizaki T, Yamaguchi H, Shinzawa-Itoh K, Nakashima R, Yaono R, Yoshikawa S: **Structures of metal sites of oxidized bovine heart cytochrome c oxidase at 2.8 Å.** *Science* 1995, **269**:1069-1074.
7. Tsukihara T, Aoyama H, Yamashita E, Tomizaki T, Yamaguchi H, Shinzawa-Itoh K, Nakashima R, Yaono R, Yoshikawa S: **The whole structure of the 13-subunit oxidized cytochrome c oxidase at 2.8 Å.** *Science* 1996, **272**:1136-1144.

The first complete crystal structure of the mitochondrial respiratory Complex IV from bovine heart, an important breakthrough in the structural biology of mitochondrial respiratory complexes.

8. Ostermeier C, Harrenga A, Ermiler U, Michel H: **Structure at 2.7 Å resolution of the *Paracoccus denitrificans* two-subunit cytochrome c oxidase complexed with an antibody FV fragment.** *Proc Natl Acad Sci U S A* 1997, **94**:10547-10553.
9. Kannt A, Lancaster CR, Michel H: **The coupling of electron transfer and proton translocation: electrostatic calculations on *Paracoccus denitrificans* cytochrome c oxidase.** *Biophys J* 1998, **74**:708-721.
10. Yoshikawa S, Shinzawa-Itoh K, Nakashima R, Yaono R, Yamashita E, Inoue N, Yao M, Fei MJ, Libeu CP, Mizushima T *et al.*: **Redox-coupled crystal structural changes in bovine heart cytochrome c oxidase.** *Science* 1998, **280**:1723-1729.
Molecular mechanism of proton translocation coupling for the mitochondrial respiratory Complex IV, suggesting the third proton channel, the H-pathway.
11. Harrenga A, Michel H: **The cytochrome c oxidase from *Paracoccus denitrificans* does not change the metal center ligation upon reduction.** *J Biol Chem* 1999, **274**:33296-33299.
12. Svensson-Ek M, Abramson J, Larsson G, Tornroth S, Brzezinski P, Iwata S: **The X-ray crystal structures of wild-type and EQ(I-286) mutant cytochrome c oxidases from *Rhodobacter sphaeroides*.** *J Mol Biol* 2002, **321**:329-339.
13. Tsukihara T, Shimokata K, Katayama Y, Shimada H, Muramoto K, Aoyama H, Mochizuki M, Shinzawa-Itoh K, Yamashita E, Yao M *et al.*: **The low-spin heme of cytochrome c oxidase as the driving element of the proton-pumping process.** *Proc Natl Acad Sci U S A* 2003, **100**:15304-15309.
Molecular mechanism of proton translocation coupling for the mitochondrial respiratory Complex IV, further indicating the key role of heme a for pumping protons along the H-pathway.
14. Kaila VRI, Sharma V, Wikström M: **The identity of the transient proton loading site of the proton-pumping mechanism of cytochrome c oxidase.** *Biochim Biophys Acta (BBA): Bioenerg* 2011, **1807**:80-84.
15. Muramoto K, Hirata K, Shinzawa-Itoh K, Yoko-o S, Yamashita E, Aoyama H, Tsukihara T, Yoshikawa S: **A histidine residue acting as a controlling site for dioxygen reduction and proton pumping by cytochrome c oxidase.** *Proc Natl Acad Sci U S A* 2007, **104**:7881-7886.
16. Aoyama H, Muramoto K, Shinzawa-Itoh K, Hirata K, Yamashita E, Tsukihara T, Ogura T, Yoshikawa S: **A peroxide bridge between Fe and Cu ions in the O₂ reduction site of fully oxidized cytochrome c oxidase could suppress the proton pump.** *Proc Natl Acad Sci U S A* 2009, **106**:2165-2169.
17. Muramoto K, Ohta K, Shinzawa-Itoh K, Kanda K, Taniguchi M, Nabekura H, Yamashita E, Tsukihara T, Yoshikawa S: **Bovine cytochrome c oxidase structures enable O₂ reduction with minimization of reactive oxygens and provide a proton-pumping gate.** *Proc Natl Acad Sci U S A* 2010, **107**:7740-7745.
18. Kamiya K, Boero M, Tateno M, Shiraishi K, Oshiyama A: **Possible mechanism of proton transfer through peptide groups in the H-pathway of the bovine cytochrome c oxidase.** *J Am Chem Soc* 2007, **129**:9663-9673.
19. Belevich I, Verkhovskiy MI, Wikstrom M: **Proton-coupled electron transfer drives the proton pump of cytochrome c oxidase.** *Nature* 2006, **440**:829-832.
20. Egawa T, Yeh SR, Rousseau DL: **Redox-controlled proton gating in bovine cytochrome c oxidase.** *PLoS ONE* 2013, **8**:e63669.
21. Sugitani R, Medvedev ES, Stuchebrukhov AA: **Theoretical and computational analysis of the membrane potential generated by cytochrome c oxidase upon single electron injection into the enzyme.** *Biochim Biophys Acta* 2008, **1777**:1129-1139.
22. Belevich I, Bloch DA, Belevich N, Wikström M, Verkhovskiy MI: **Exploring the proton pump mechanism of cytochrome c oxidase in real time.** *Proc Natl Acad Sci U S A* 2007, **104**:2685-2690.
23. Xia D, Yu CA, Kim H, Xia JZ, Kachurin AM, Zhang L, Yu L, Deisenhofer J: **Crystal structure of the cytochrome bc₁ complex from bovine heart mitochondria.** *Science* 1997, **277**:60-66.
24. Iwata S, Lee JW, Okada K, Lee JK, Iwata M, Rasmussen B, Link TA, Ramaswamy S, Jap BK: **Complete structure of the 11-subunit bovine mitochondrial cytochrome bc₁ complex.** *Science* 1998, **281**:64-71.
The first crystal structure of the mitochondrial respiratory Complex III from bovine heart.
25. Zhang Z, Huang L, Shulmeister VM, Chi YI, Kim KK, Hung LW, Crofts AR, Berry EA, Kim SH: **Electron transfer by domain movement in cytochrome bc₁.** *Nature* 1998, **392**:677-684.
Molecular mechanism of electron transfer for the mitochondrial respiratory Complex III, observing the movement of ISP subunit and suggesting its important role for bifurcating electron to heme c₁.
26. Lange C, Hunte C: **Crystal structure of the yeast cytochrome bc₁ complex with its bound substrate cytochrome c.** *Proc Natl Acad Sci U S A* 2002, **99**:2800-2805.
The interaction interface between bc₁ complex and cytochrome c was identified, revealing the electron transfer pathway from heme c₁ to heme c.
27. Gao X, Wen X, Yu C, Esser L, Tsao S, Quinn B, Zhang L, Yu L, Xia D: **The crystal structure of mitochondrial cytochrome bc₁ in complex with famoxadone: the role of aromatic-aromatic interaction in inhibition.** *Biochemistry* 2002, **41**:11692-11702.
28. Gao X, Wen X, Esser L, Quinn B, Yu L, Yu CA, Xia D: **Structural basis for the quinone reduction in the bc₁ complex: a comparative analysis of crystal structures of mitochondrial cytochrome bc₁ with bound substrate and inhibitors at the Qi site.** *Biochemistry* 2003, **42**:9067-9080.
29. Palsdottir H, Lojero CG, Trumpower BL, Hunte C: **Structure of the yeast cytochrome bc₁ complex with a hydroxyquinone anion Qo site inhibitor bound.** *J Biol Chem* 2003, **278**:31303-31311.
30. Esser L, Gong X, Yang S, Yu L, Yu CA, Xia D: **Surface-modulated motion switch: capture and release of iron-sulfur protein in the cytochrome bc₁ complex.** *Proc Natl Acad Sci U S A* 2006, **103**:13045-13050.
31. Lenaz G: **A critical appraisal of the mitochondrial coenzyme Q pool.** *FEBS Lett* 2001, **509**:151-155.
32. Mitchell P: **Protonmotive redox mechanism of the cytochrome b-c₁ complex in the respiratory chain: protonmotive ubiquinone cycle.** *FEBS Lett* 1975, **56**:1-6.
33. Mitchell P: **The protonmotive Q cycle: a general formulation.** *FEBS Lett* 1975, **59**:137-139.
34. Solmaz SR, Hunte C: **Structure of complex III with bound cytochrome c in reduced state and definition of a minimal core interface for electron transfer.** *J Biol Chem* 2008, **283**:17542-17549.
35. Osyczka A, Moser CC, Dutton PL: **Fixing the Q cycle.** *Trends Biochem Sci* 2005, **30**:176-182.
An informative review upon discussing the possible mechanism of avoiding the electron transfer short circuit of mitochondrial respiratory Complex III.
36. Mulikdjanian AY: **Activated Q-cycle as a common mechanism for cytochrome bc₁ and cytochrome b₆f complexes.** *Biochim Biophys Acta* 2010, **1797**:1858-1868.
37. Smirnov AY, Nori F: **Modeling the Q-cycle mechanism of transmembrane energy conversion.** *Phys Biol* 2012, **9**:016011.
38. Malnoe A, Wollman FA, de Vitry C, Rappaport F: **Photosynthetic growth despite a broken Q-cycle.** *Nat Commun* 2011, **2**:301.
39. Yankovskaya V, Horsefield R, Tornroth S, Luna-Chavez C, Miyoshi H, Leger C, Byrne B, Cecchini G, Iwata S: **Architecture of succinate dehydrogenase and reactive oxygen species generation.** *Science* 2003, **299**:700-704.
The first crystal structure of the prokaryotic version of Complex II.
40. Sun F, Huo X, Zhai Y, Wang A, Xu J, Su D, Bartlam M, Rao Z: **Crystal structure of mitochondrial respiratory membrane protein complex II.** *Cell* 2005, **121**:1043-1057.

The first crystal structure of the mitochondrial respiratory complex II from porcine heart, showing the ubiquinone binding site at the proximal side.

41. Huang LS, Sun G, Cobessi D, Wang AC, Shen JT, Tung EY, Anderson VE, Berry EA: **3-Nitropropionic acid is a suicide inhibitor of mitochondrial respiration that, upon oxidation by complex II, forms a covalent adduct with a catalytic base arginine in the active site of the enzyme.** *J Biol Chem* 2006, **281**:5965-5972.
 42. Kluckova K, Bezawork-Geleta A, Rohlena J, Dong L, Neuzil J: **Mitochondrial complex II, a novel target for anti-cancer agents.** *Biochim Biophys Acta* 2013, **1827**:552-564.
 43. Iverson TM, Luna-Chavez C, Cecchini G, Rees DC: **Structure of the *Escherichia coli* fumarate reductase respiratory complex.** *Science* 1999, **284**:1961-1966.
 44. Lancaster CR, Kroger A, Auer M, Michel H: **Structure of fumarate reductase from *Wolinella succinogenes* at 2.2 Å resolution.** *Nature* 1999, **402**:377-385.
 45. Lemos RS, Fernandes AS, Pereira MM, Gomes CM, Teixeira M: **Quinol:fumarate oxidoreductases and succinate:quinone oxidoreductases: phylogenetic relationships, metal centres and membrane attachment.** *Biochim Biophys Acta* 2002, **1553**:158-170.
 46. Ruprecht J, Yankovskaya V, Maklashina E, Iwata S, Cecchini G: **Structure of *Escherichia coli* succinate:quinone oxidoreductase with an occupied and empty quinone-binding site.** *J Biol Chem* 2009, **284**:29836-29846.
 47. Horsefield R, Yankovskaya V, Sexton G, Whittingham W, Shiomi K, Omura S, Byrne B, Cecchini G, Iwata S: **Structural and computational analysis of the quinone-binding site of complex II (succinate-ubiquinone oxidoreductase): a mechanism of electron transfer and proton conduction during ubiquinone reduction.** *J Biol Chem* 2006, **281**:7309-7316.
 48. Iverson TM, Luna-Chavez C, Croal LR, Cecchini G, Rees DC: **Crystallographic studies of the *Escherichia coli* quinol-fumarate reductase with inhibitors bound to the quinol-binding site.** *J Biol Chem* 2002, **277**:16124-16130.
 49. Zhou Q, Zhai Y, Lou J, Liu M, Pang X, Sun F: **Thiabendazole inhibits ubiquinone reduction activity of mitochondrial respiratory complex II via a water molecule mediated binding feature.** *Protein Cell* 2011, **2**:531-542.
 50. Yu L, Xu JX, Haley PE, Yu CA: **Properties of bovine heart mitochondrial cytochrome b560.** *J Biol Chem* 1987, **262**:1137-1143.
 51. Sazanov LA, Hinchliffe P: **Structure of the hydrophilic domain of respiratory complex I from *Thermus thermophilus*.** *Science* 2006, **311**:1430-1436.
- The first breakthrough in the structural studies of respiratory Complex I, solving the crystal structure of the hydrophilic part of prokaryotic Complex I and revealing the arrangement of its embedded prosthetic groups.
52. Efremov RG, Baradaran R, Sazanov LA: **The architecture of respiratory complex I.** *Nature* 2010, **465**:441-445.
 53. Efremov RG, Sazanov LA: **Structure of the membrane domain of respiratory complex I.** *Nature* 2011, **476**:414-420.
 54. Baradaran R, Berrisford JM, Minhas GS, Sazanov LA: **Crystal structure of the entire respiratory complex I.** *Nature* 2013, **494**:443-448.
- The most recent breakthrough about the complete crystal structure of prokaryotic Complex I, suggesting a single-step reversible allosteric mechanism for coupled proton translocations.
55. Hunte C, Zickermann V, Brandt U: **Functional modules and structural basis of conformational coupling in mitochondrial complex I.** *Science* 2010, **329**:448-451.
 56. Schapira AH: **Human complex I defects in neurodegenerative diseases.** *Biochim Biophys Acta* 1998, **1364**:261-270.
 57. Dawson TM, Dawson VL: **Molecular pathways of neurodegeneration in Parkinson's disease.** *Science* 2003, **302**:819-822.
 58. Carroll J, Fearnley IM, Skehel JM, Shannon RJ, Hirst J, Walker JE: **Bovine complex I is a complex of 45 different subunits.** *J Biol Chem* 2006, **281**:32724-32727.
 59. Balsa E, Marco R, Perales-Clemente E, Szklarczyk R, Calvo E, Landazuri MO, Enriquez JA: **NDUFA4 is a subunit of complex IV of the mammalian electron transport chain.** *Cell Metab* 2012, **16**:378-386.
 60. Hirst J, Carroll J, Fearnley IM, Shannon RJ, Walker JE: **The nuclear encoded subunits of complex I from bovine heart mitochondria.** *Biochim Biophys Acta* 2003, **1604**:135-150.
 61. Sazanov LA, Carroll J, Holt P, Toime L, Fearnley IM: **A role for native lipids in the stabilization and two-dimensional crystallization of the *Escherichia coli* NADH-ubiquinone oxidoreductase (complex I).** *J Biol Chem* 2003, **278**:19483-19491.
 62. Walker JE: **The NADH:ubiquinone oxidoreductase (complex I) of respiratory chains.** *Q Rev Biophys* 1992, **25**:253-324.
 63. Yagi T, Matsuno-Yagi A: **The proton-translocating NADH-ubiquinone oxidoreductase in the respiratory chain: the secret unlocked.** *Biochemistry* 2003, **42**:2266-2274.
 64. Sazanov LA: **Respiratory complex I: mechanistic and structural insights provided by the crystal structure of the hydrophilic domain.** *Biochemistry* 2007, **46**:2275-2288.
 65. Brandt U: **Energy converting NADH:quinone oxidoreductase (complex I).** *Annu Rev Biochem* 2006, **75**:69-92.
 66. Efremov RG, Sazanov LA: **Respiratory complex I: 'steam engine' of the cell?** *Curr Opin Struct Biol* 2011, **21**:532-540.
 67. Angerer H, Zwicker K, Wumaier Z, Sokolova L, Heide H, Steger M, Kaiser S, Nubel E, Brutschy B, Radermacher M *et al.*: **A scaffold of accessory subunits links the peripheral arm and the distal proton-pumping module of mitochondrial complex I.** *Biochem J* 2011, **437**:279-288.
 68. Peng G, Fritzsche G, Zickermann V, Schagger H, Mentele R, Lottspeich F, Bostina M, Radermacher M, Huber R, Stetter KO *et al.*: **Isolation, characterization and electron microscopic single particle analysis of the NADH:ubiquinone oxidoreductase (complex I) from the hyperthermophilic eubacterium *Aquifex aeolicus*.** *Biochemistry* 2003, **42**:3032-3039.
 69. Guenebaut V, Schlitt A, Weiss H, Leonard K, Friedrich T: **Consistent structure between bacterial and mitochondrial NADH:ubiquinone oxidoreductase (complex I).** *J Mol Biol* 1998, **276**:105-112.
 70. Bottcher B, Scheide D, Hesterberg M, Nagel-Steger L, Friedrich T: **A novel, enzymatically active conformation of the *Escherichia coli* NADH:ubiquinone oxidoreductase (complex I).** *J Biol Chem* 2002, **277**:17970-17977.
 71. Leonard K, Haiker H, Weiss H: **Three-dimensional structure of NADH:ubiquinone reductase (complex I) from *Neurospora* mitochondria determined by electron microscopy of membrane crystals.** *J Mol Biol* 1987, **194**:277-286.
 72. Hofhaus G, Weiss H, Leonard K: **Electron microscopic analysis of the peripheral and membrane parts of mitochondrial NADH dehydrogenase (complex I).** *J Mol Biol* 1991, **221**:1027-1043.
 73. Guenebaut V, Vincentelli R, Mills D, Weiss H, Leonard KR: **Three-dimensional structure of NADH-dehydrogenase from *Neurospora crassa* by electron microscopy and conical tilt reconstruction.** *J Mol Biol* 1997, **265**:409-418.
 74. Radermacher M, Ruiz T, Clason T, Benjamin S, Brandt U, Zickermann V: **The three-dimensional structure of complex I from *Yarrowia lipolytica*: a highly dynamic enzyme.** *J Struct Biol* 2006, **154**:269-279.
 75. Grigorieff N: **Three-dimensional structure of bovine NADH:ubiquinone oxidoreductase (complex I) at 22 Å in ice.** *J Mol Biol* 1998, **277**:1033-1046.
 76. Clason T, Ruiz T, Schagger H, Peng G, Zickermann V, Brandt U, Michel H, Radermacher M: **The structure of eukaryotic and prokaryotic complex I.** *J Struct Biol* 2010, **169**:81-88.
 77. Baradaran R, Berrisford JM, Minhas GS, Sazanov LA: **Crystal structure of the entire respiratory complex I.** *Nature* 2013 <http://dx.doi.org/10.1038/nature11871>.

78. Ohnishi T, Nakamaru-Ogiso E, Ohnishi ST: **A new hypothesis on the simultaneous direct and indirect proton pump mechanisms in NADH-quinone oxidoreductase (complex I).** *FEBS Lett* 2010, **584**:4131-4137.
79. Ohnishi ST, Salerno JC, Ohnishi T: **Possible roles of two quinone molecules in direct and indirect proton pumps of bovine heart NADH-quinone oxidoreductase (complex I).** *Biochim Biophys Acta* 2010, **1797**:1891-1893.
80. Ohnishi T, Johnson JE Jr, Yano T, Lohbrutto R, Widger WR: **Thermodynamic and EPR studies of slowly relaxing ubisemiquinone species in the isolated bovine heart complex I.** *FEBS Lett* 2005, **579**:500-506.
81. Brandt U: **A two-state stabilization-change mechanism for proton-pumping complex I.** *Biochim Biophys Acta* 2011, **1807**:1364-1369.
82. Efremov RG, Sazanov LA: **The coupling mechanism of respiratory complex I – a structural and evolutionary perspective.** *Biochim Biophys Acta* 2012, **1817**:1785-1795.
A proposed single-step reversible coupling mechanism of respiratory complex I. In this paper, the authors, for the first time, raised the prediction that it is the negatively charged head group of ubiquinol that triggers the conformational changes of the complex.
83. Boekema EJ, Braun HP: **Supramolecular structure of the mitochondrial oxidative phosphorylation system.** *J Biol Chem* 2007, **282**:1-4.
84. Schafer E, Seelert H, Reifschneider NH, Krause F, Dencher NA, Vonck J: **Architecture of active mammalian respiratory chain supercomplexes.** *J Biol Chem* 2006, **281**:15370-15375.
85. Dudkina NV, Eubel H, Keegstra W, Boekema EJ, Braun HP: **Structure of a mitochondrial supercomplex formed by respiratory-chain complexes I and III.** *Proc Natl Acad Sci U S A* 2005, **102**:3225-3229.
86. Wittig I, Braun HP, Schagger H: **Blue native PAGE.** *Nat Protoc* 2006, **1**:418-428.
87. Wittig I, Schagger H: **Advantages and limitations of clear-native PAGE.** *Proteomics* 2005, **5**:4338-4346.
88. Schafer E, Dencher NA, Vonck J, Parcej DN: **Three-dimensional structure of the respiratory chain supercomplex I1III2IV1 from bovine heart mitochondria.** *Biochemistry* 2007, **46**:12579-12585.
89. Althoff T, Mills DJ, Popot JL, Kuhlbrandt W: **Arrangement of electron transport chain components in bovine mitochondrial supercomplex I1III2IV1.** *EMBO J* 2011, **30**:4652-4664.
Electron microscopic study of the mitochondrial supra-complex comprising complexes I, III and IV.
90. Dudkina NV, Kudryashev M, Stahlberg H, Boekema EJ: **Interaction of complexes I, III, and IV within the bovine respirasome by single particle cryoelectron tomography.** *Proc Natl Acad Sci U S A* 2011, **108**:15196-15200.
Electron microscopic study of the mitochondrial supra-complex comprising complexes I, III and IV.
91. Eubel H, Heinemeyer J, Sunderhaus S, Braun HP: **Respiratory chain supercomplexes in plant mitochondria.** *Plant Physiol Biochem* 2004, **42**:937-942.
92. Heinemeyer J, Braun HP, Boekema EJ, Kouril R: **A structural model of the cytochrome C reductase/oxidase supercomplex from yeast mitochondria.** *J Biol Chem* 2007, **282**:12240-12248.
93. Bazan S, Mileykovskaya E, Mallampalli VK, Heacock P, Sparagna GC, Dowhan W: **Cardiolipin-dependent reconstitution of respiratory supercomplexes from purified *Saccharomyces cerevisiae* complexes III and IV.** *J Biol Chem* 2013, **288**:401-411.
94. Lenaz G, Genova ML: **Supramolecular organisation of the mitochondrial respiratory chain: a new challenge for the mechanism and control of oxidative phosphorylation.** *Adv Exp Med Biol* 2012, **748**:107-144.